

# Quarkonia production and dissociation in Pb+Pb collisions

Vineet Kumar<sup>1,2</sup> and Prashant Shukla<sup>1,2,\*</sup>

<sup>1</sup>*Nuclear Physics Division, Bhabha Atomic Research Center, Mumbai, India*

<sup>2</sup>*Homi Bhabha National Institute, Anushakti Nagar, Mumbai, India*

(Dated: December 22, 2015)

## Abstract

We calculate the high  $p_T$  quarkonia production using NRQCD method. Different methods of quarkonia suppression are used to explain the high  $p_T$  quarkonia suppression observed by CMS in LHC

PACS numbers: 12.38.Mh, 24.85.+p, 25.75.-q

Keywords: quark-gluon plasma, quarkonia, suppression, regeneration

---

\* pshukla@barc.gov.in

## I. INTRODUCTION

Heavy-ion collisions at relativistic energies are performed to create and characterize quark gluon plasma (QGP), a phase of strongly-interacting matter at high energy density where quarks and gluons are no longer bound within hadrons. The quarkonia states ( $J/\psi$  and  $\Upsilon$ ) have been some of the most popular tools since their suppression was proposed as a signal of QGP formation [1]. The understanding of these probes has evolved substantially via measurements through three generations of experiments: the SPS (at CERN), RHIC (at BNL) and the LHC (at CERN) and by a great deal of theoretical activity. (For recent reviews see Refs. [2–4].) Quarkonia are produced early in the heavy-ion collisions and, if they evolve through the deconfined medium, their yields should be suppressed in comparison with those in  $pp$  collisions. The first such measurement was the ‘anomalous’  $J/\psi$  suppression discovered at the SPS which was considered to be a hint of QGP formation. The RHIC measurements showed almost the same suppression at a much higher energy contrary to expectation [4, 5]. Such an observation was consistent with the scenario that, at higher collision energies, the expected greater suppression is compensated by  $J/\psi$  regeneration through recombination of two independently-produced charm quarks [6].

In this paper, we calculate  $J/\psi$  and  $\Upsilon$  production and suppression

## II. QUARKONIA PRODUCTION IN P+P COLLISIONS

In this section we describe the production of quarkonia at high transverse momenta in p+p collisions. The factorization formalism of the NRQCD provides a theoretical framework for studying the heavy quarkonium production and decay. Under NRQCD the cross-section for direct production of a resonance  $H$  in a collision of particle  $A$  and  $B$  can be expressed in factorized form

$$E \frac{d^3\sigma^{ab \rightarrow cd}}{d^3p}({}^{(2S+1)}L_J) = \sum_{a,b} \int \int dx_a dx_b G_{a/A}(x_a, \mu_F^2) G_{b/B}(x_b, \mu_F^2) \frac{\hat{s}}{\pi} \frac{d\sigma}{d\hat{t}} (ab \rightarrow {}^{(2S+1)}L_J c) \otimes \delta(\hat{s} + \hat{t} + \hat{u} - M^2) \quad (1)$$

where,  $G_{a/A}(G_{b/B})$  is the parton distribution function (PDF) of the incoming parton  $a(b)$  in the incident hadron  $A(B)$ , which depends on the momentum fraction  $x_a(x_b)$  and the factorization scale  $\mu_F$  as well as on the renormalization scale  $\mu_R$ . However, as we have

chosen  $\mu_F = \mu_R$ , in our case PDFs are function of  $x$  and  $\mu_F$  only. The short distance contribution  $d\sigma/d\hat{t}$  can be calculated within the framework of perturbative QCD (pQCD).  $(ab \rightarrow^{(2S+1)} L_J c)$  are the nonperturbative LDMEs and can be estimated by comparison with experimental measurements.

Using the invariant relation

$$E \frac{d^3\sigma}{d^3p} = \frac{d^2\sigma}{2\pi p_T dp_T dy} \quad (2)$$

the cross section shown in eq. 1 can be written in the terms of resonance transeverse momentum and rapidity

$$\begin{aligned} \frac{d^2\sigma^{ab \rightarrow cd}}{dp_T dy} ({}^{(2S+1)} L_J) &= \sum_{a,b} \int \int dx_a dx_b G_{a/A}(x_a, \mu_F^2) G_{b/B}(x_b, \mu_F^2) \times 2\hat{s} p_T \frac{d\sigma}{d\hat{t}} \\ & (ab \rightarrow^{(2S+1)} L_J c) \otimes \delta(\hat{s} + \hat{t} + \hat{u} - M^2) \end{aligned} \quad (3)$$

At this stage, the integration upon  $x_b$  can be performed using the properties delta function. To solve the integration we have to express the  $\hat{s}$ ,  $\hat{t}$ , and  $\hat{u}$  in terms of  $x_a$ ,  $x_b$ , resonance transeverse momentum  $p_T$  and rapidity  $y$ . The dominant processes in evaluating the differential yields of heavy mesons as a function of  $p_T$  are the  $2 \rightarrow 2$  processes of the kind  $g + q \rightarrow H + q$ ,  $q + \bar{q} \rightarrow H + g$  and  $g + g \rightarrow H + g$ , where  $H$  refers to the heavy meson. We label the process generically as  $a + b \rightarrow c + d$ , where  $a$  and  $b$  are light incident partons,  $c$  refers to  $H$  and  $d$  is a light final-state parton. For these kind processes following are the relations between  $\hat{s}$ ,  $\hat{t}$ ,  $\hat{u}$  and meson variables

$$\begin{aligned} \hat{s} &= x_a x_b s \\ \hat{t} &= M^2 - x_a \sqrt{s} m_T e^{-y} \\ \hat{u} &= M^2 - x_b \sqrt{s} m_T e^y \end{aligned} \quad (4)$$

Writing down  $\hat{s} + \hat{t} + \hat{u} - M^2$  and solving for  $x_b$  we obtain

$$x_b = \frac{1}{\sqrt{s}} \frac{x_a \sqrt{s} m_T e^{-y} - m_H^2}{x_a \sqrt{s} - m_T e^y}. \quad (5)$$

The double differential cross-section upon  $p_T$  and  $y$  takes the following form

$$\frac{d^2\sigma^{ab \rightarrow cd}}{dp_T dy} = \int_{x_a^{min}}^1 dx_a G_{a/A}(x_a, \mu_F^2) G_{b/B}(x_b, \mu_F^2) \times 2p_T \frac{x_a x_b}{x_a - \frac{m_T}{\sqrt{s}} e^y} \frac{d\sigma}{d\hat{t}}(ab \rightarrow cd), \quad (6)$$

where,  $\sqrt{s}$  being the total energy in the centre-of-mass and  $y$  is the rapidity of the  $Q\bar{Q}$  pair. The minimum value of  $x_a$  is

$$x_{a\min} = \frac{1}{\sqrt{s}} \frac{\sqrt{s} m_T e^y - m_H^2}{\sqrt{s} - m_T e^{-y}}. \quad (7)$$

The invariant differential cross-section is given by

$$\frac{d\sigma}{d\hat{t}} = \frac{|\mathcal{M}|^2}{16\pi\hat{s}^2}, \quad (8)$$

where  $\hat{s}$  and  $\hat{t}$  are the parton level Mandelstam variables.  $|\mathcal{M}|^2$  is the feynman squared amplitude, averaged on the initial spin and color degrees of freedom and summed over the final ones. In our numerical computation, we use CTEQ6M [7] for the parton distribution functions.

The LDMEs are predicted to scale with a definite power of the relative velocity  $v$  of the heavy constituents inside  $Q\bar{Q}$  bound states. In the limit  $v \ll 1$ , the production of quarkonium is based on the  $^3S_1^{[1]}$  and  $^3P_J^{[1]}$  ( $J = 0, 1, 2$ ) CS states and  $^1S_0^{[8]}$ ,  $^3S_1^{[8]}$  and  $^3P_J^{[8]}$  CO states. In our calculations, we used the expressions for the short distance CS cross-sections given in Refs. [10–12] and the CO cross-sections given in Refs. [13, 14].

In this section we calculate the  $p_T$  distribution of  $J/\psi$ ,  $\psi(2S)$  and  $\Upsilon(nS)$  mesons in  $p-p$  collisions at LHC energies. For  $J/\psi$  production in  $p-p$  collisions, three sources need to be considered: direct  $J/\psi$  production, feed-down contributions to the  $J/\psi$  from the decay of heavier charmonium states, predominantly from  $\psi(2S)$ ,  $\chi_{c0}$ ,  $\chi_{c1}$  and  $\chi_{c2}$  and  $J/\psi$  from  $B$  hadron decays. The sum of the first two sources is called "prompt  $J/\psi$ " and the third source will be called " $J/\psi$  from  $B$ ". On the other hand,  $\psi(2S)$  has no significant feed-down contributions from higher mass states. We call this direct contribution as "prompt  $\psi(2S)$ " to be consistent with the experiments. The other source to  $\psi(2S)$  production is from  $B$  hadron decays and we call it " $\psi(2S)$  from  $B$ ". The sum of the prompt  $J/\psi(\psi(2S))$  and  $J/\psi(\psi(2S))$  from  $B$  will be called "inclusive  $J/\psi(\psi(2S))$ ". Similar terminology is used for  $\Upsilon$  states, only difference is that we do not have any contribution from open T mesons.

NRQCD provides a systematic procedure to compute any quantity as an expansion in the relative velocity  $v$  of the heavy quarks in the meson. For example, the wavefunction of the  $J/\psi$  meson (analogous expressions hold for the  $\psi(2S)$ ,  $\Upsilon(1S)$ ,  $\Upsilon(2S)$  and  $\Upsilon(3S)$ ) is written as

$$\begin{aligned} |J/\psi\rangle = & |Q\bar{Q}([{}^3S_1]_1)\rangle + \mathcal{O}(v)|Q\bar{Q}([{}^1S_0]_{8g})\rangle + \mathcal{O}(v^2)|Q\bar{Q}([{}^3S_1]_{8gg})\rangle \\ & + \mathcal{O}(v^1)|Q\bar{Q}([{}^3P_0]_{8g})\rangle + \mathcal{O}(v^1)|Q\bar{Q}([{}^3P_1]_{8g})\rangle + \mathcal{O}(v^1)|Q\bar{Q}([{}^3P_2]_{8g})\rangle + \dots \end{aligned} \quad (9)$$

The differential cross section for the direct production of  $J/\psi$  can be written as the sum

of the contributions,

$$\begin{aligned}
d\sigma(J/\psi) = & d\sigma(Q\bar{Q}([{}^3S_1]_1))\langle\mathcal{O}(Q\bar{Q}([{}^3S_1]_1) \rightarrow J/\psi)\rangle + d\sigma(Q\bar{Q}([{}^1S_0]_8))\langle\mathcal{O}(Q\bar{Q}([{}^1S_0]_8) \rightarrow J/\psi)\rangle \\
& + d\sigma(Q\bar{Q}([{}^3S_1]_8))\langle\mathcal{O}(Q\bar{Q}([{}^3S_1]_8) \rightarrow J/\psi)\rangle + d\sigma(Q\bar{Q}([{}^3P_0]_8))\langle\mathcal{O}(Q\bar{Q}([{}^3P_0]_8) \rightarrow J/\psi)\rangle \\
& + d\sigma(Q\bar{Q}([{}^3P_1]_8))\langle\mathcal{O}(Q\bar{Q}([{}^3P_1]_8) \rightarrow J/\psi)\rangle + d\sigma(Q\bar{Q}([{}^3P_2]_8))\langle\mathcal{O}(Q\bar{Q}([{}^3P_2]_8) \rightarrow J/\psi)\rangle + \cdots,
\end{aligned} \tag{10}$$

where the quantity in the brackets  $[ \ ]$  represents the angular momentum quantum numbers of the  $Q\bar{Q}$  pair in the Fock expansion. The subscript on  $[ \ ]$  refers to the color structure of the  $Q\bar{Q}$  pair, 1 being the color-singlet and 8 being the color-octet. The dots represent terms which contribute at higher powers of  $v$ . The short distance cross sections  $d\sigma(Q\bar{Q})$  correspond to the production of a  $Q\bar{Q}$  pair in a particular color and spin configuration, while the long distance matrix element  $\langle\mathcal{O}(Q\bar{Q}) \rightarrow J/\psi\rangle$  corresponds to the probability of the  $Q\bar{Q}$  state to convert to the quarkonium wavefunction. This probability includes any necessary prompt emission of soft gluons to prepare a color neutral system that matches onto the corresponding Fock component of the quarkonium wavefunction.

Power counting rules tell us that contributions from the color-octet matrix elements in Eq. 10 are suppressed by  $v^4$  compared to the color singlet matrix elements. More specifically,

$$\begin{aligned}
\langle\mathcal{O}(Q\bar{Q}([{}^3S_1]_1) \rightarrow J/\psi)\rangle &= \mathcal{O}(m_Q^3 v^3), \\
\langle\mathcal{O}(Q\bar{Q}([{}^3S_1]_8) \rightarrow J/\psi)\rangle &= \mathcal{O}(m_Q^3 v^7), \\
\langle\mathcal{O}(Q\bar{Q}([{}^1S_0]_8) \rightarrow J/\psi)\rangle &= \mathcal{O}(m_Q^3 v^7), \\
\langle\mathcal{O}(Q\bar{Q}([{}^3P_J]_8) \rightarrow J/\psi)\rangle &= \mathcal{O}(m_Q^5 v^7).
\end{aligned} \tag{11}$$

These operators are multiplied by the short distance differential cross sections, which are related to the probability to create  $Q\bar{Q}$  pairs in specific quantum states. Since these are short distance operators, they can be calculated in perturbation theory. We use the expressions for the short distance color-singlet cross sections given in [10, 11] and the color-octet cross sections given in [13–15].

The case of the  $p$ -wave bound states ( $\chi_{c0}$ ,  $\chi_{c1}$ , and  $\chi_{c2}$ , sometimes collectively referred to as  $\chi_{cJ}$ , and the corresponding states of the  $b$  quark) is slightly different. The wavefunction

of  $\chi_c$  states can be written as

$$\begin{aligned}
|\chi_{cJ}\rangle = & |Q\bar{Q}([{}^3P_J]_1)\rangle + \mathcal{O}(v)|Q\bar{Q}([{}^3S_1]_8g)\rangle + \mathcal{O}(v^2)|Q\bar{Q}([{}^1S_0]_8g)\rangle + \mathcal{O}(v)|Q\bar{Q}([{}^3D_J]_8g)\rangle \\
& + \mathcal{O}(v^2)|Q\bar{Q}([{}^1P_1]_8g)\rangle + \mathcal{O}(v^2)|Q\bar{Q}([{}^3P_J]_8gg)\rangle + \dots
\end{aligned} \tag{12}$$

The color-singlet state  $Q\bar{Q}([{}^3P_J]_1)$  and the color-octet state  $Q\bar{Q}([{}^3S_1]_8)$  contribute to the same order in  $v$  because of the angular momentum barrier for  $p$ -wave states, and hence both need to be included for a consistent calculation in  $v$ . For the calculation of the production cross section, we consistently take the contributions to the lowest order in  $v$ . For example the  $\chi_c$  contribution is

$$d\sigma(\chi_{cJ}) = d\sigma(Q\bar{Q}([{}^3P_J]_1))\langle\mathcal{O}(Q\bar{Q}([{}^3P_J]_1) \rightarrow \chi_{cJ})\rangle + d\sigma(Q\bar{Q}([{}^3S_1]_8))\langle\mathcal{O}(Q\bar{Q}([{}^3S_1]_8) \rightarrow \chi_{cJ})\rangle + \dots \tag{13}$$

Similar expressions hold for the  $\chi_b(1P)$ ,  $\chi_b(2P)$  and  $\chi_b(3P)$  mesons. The expressions for the short distance coefficients are given in [13]. The scaling of the matrix elements is given as

$$\begin{aligned}
\langle\mathcal{O}(Q\bar{Q}([{}^3P_J]_1) \rightarrow \chi_{cJ})\rangle &= \mathcal{O}(m_Q^5 v^5) , \\
\langle\mathcal{O}(Q\bar{Q}([{}^3S_1]_8) \rightarrow \chi_{cJ})\rangle &= \mathcal{O}(m_Q^5 v^5) .
\end{aligned} \tag{14}$$

Therefore we need the color-singlet and color-octet matrix elements to obtain theoretical results for the production of quarkonia at RHIC and LHC energies.

### A. Feed-down contributions

For the net production of  $J/\psi$  we consider the direct contribution, and feed-down contributions from  $\chi_{c0}(1P)$ ,  $\chi_{c1}(1P)$ ,  $\chi_{c2}(1P)$  and  $\psi(2S)$ . The relevant branching fractions are given in Table I,

$B$  hadrons can also decay to  $J/\psi(\psi(2S))$  with a net effective branching fraction  $B(H_b \rightarrow J/\psi + X)_{\text{eff}} = 1.16(2.83) \times 10^{-2}$  [23]. In particular, at high  $p_T$ , the contribution to the inclusive yield from the decay of  $B$ -hadrons is substantial, and can possibly even dominate production.

The analysis of  $\Upsilon(1S)$  production and feed-down contributions is very similar to the analysis for  $J/\psi$ . Following [13, 14] we consider states up to  $n = 3$ . For the  $\Upsilon(3S)$ , we consider only the direct contribution. For  $\Upsilon(2S)$ , we consider feed-down from  $\Upsilon(2S)$  and

meson from	to $\chi_{c0}$	to $\chi_{c1}$	to $\chi_{c2}$	to $J/\psi$
$\psi(2S)$	0.0962	0.092	0.0874	0.595
$\chi_{c0}$				0.0116
$\chi_{c1}$				0.344
$\chi_{c2}$				0.195

TABLE I. Relevant branching fractions for charmonia [24]

$\chi_b(2P)$ . For  $\Upsilon(1S)$  there are additional contributions from  $\Upsilon(2S)$  and  $\chi_b(1P)$ . The relevant branching fractions are given in Table II.

meson from	to $\chi_{b0}(2)$	to $\chi_{b1}(2)$	to $\chi_{b2}(2)$	to $\Upsilon(2S)$	to $\chi_{b0}(1)$	to $\chi_{b1}(1)$	to $\chi_{b2}(1)$	to $\Upsilon(1S)$
$\Upsilon(3S)$	0.131	0.126	0.059	0.199	0.003	0.0017	0.019	0.066
$\chi_{b0}(2P)$				0.046				0.009
$\chi_{b1}(2P)$				0.21				0.101
$\chi_{b2}(2P)$				0.162				0.082
$\Upsilon(2S)$					0.038	0.0715	0.069	0.267
$\chi_{b0}(1P)$								0.06
$\chi_{b1}(1P)$								0.35
$\chi_{b2}(1P)$								0.22

TABLE II. Relevant branching fractions for bottomonia [24]

## B. Long distance matrix elements (LDME) for quarkonia production

### 1. Color Singlet Matrix elements

In this work, following [13, 14] we use the values of the color-singlet operators calculated using the potential model. The expressions and the values for the color-singlet operators are

given in [13, 14, 16]. The values are obtained by solving the non-relativistic wavefunctions:

$$\begin{aligned}
\langle \mathcal{O}(c\bar{c}([{}^3S_1]_1) \rightarrow J/\psi) \rangle &= 3\langle \mathcal{O}(c\bar{c}([{}^1S_0]_1) \rightarrow J/\psi) \rangle = 3N_c \frac{|R_{n=1}(0)|^2}{2\pi} = 1.2 \text{ GeV}^3, \\
\langle \mathcal{O}(c\bar{c}([{}^3S_1]_1) \rightarrow \psi(2S)) \rangle &= 3\langle \mathcal{O}(c\bar{c}([{}^1S_0]_1) \rightarrow \psi(2S)) \rangle = 3N_c \frac{|R_{n=2}(0)|^2}{2\pi} = 0.76 \text{ GeV}^3, \\
\frac{1}{5}\langle \mathcal{O}(c\bar{c}([{}^3P_2]_1) \rightarrow \chi_{c2}(1P)) \rangle &= \frac{1}{3}\langle \mathcal{O}(c\bar{c}([{}^3P_1]_1) \rightarrow \chi_{c1}(1P)) \rangle = \\
&\langle \mathcal{O}(c\bar{c}([{}^3P_0]_1) \rightarrow \chi_{c0}(1P)) \rangle = 3N_c \frac{|R'_{n=1}(0)|^2}{2\pi} = 0.054m_{\text{charm}}^2 \text{ GeV}^3,
\end{aligned} \tag{15}$$

where  $R(0)$  is the radial wavefunction at the origin,  $R'(0)$  is the first derivative of the radial wavefunction at the origin, and  $n$  refers to the radial quantum number. We take the mass of the charm quark,  $m_{\text{charm}} = 1.4\text{GeV}$ .

The values of the color-singlet operators for bottomonia are given in [15], which we reproduce here:

$$\begin{aligned}
\langle \mathcal{O}(b\bar{b}([{}^3S_1]_1) \rightarrow \Upsilon(1S)) \rangle &= 3N_c \frac{|R_{n=1}(0)|^2}{2\pi} = 10.9 \text{ GeV}^3, \\
\langle \mathcal{O}(b\bar{b}([{}^3P_0]_1) \rightarrow \chi_{b0}(1P)) \rangle &= 3N_c \frac{|R'_{n=1}(0)|^2}{2\pi} = 0.100m_{\text{bottom}}^2 \text{ GeV}^3, \\
\langle \mathcal{O}(b\bar{b}([{}^3S_1]_1) \rightarrow \Upsilon(2S)) \rangle &= 3N_c \frac{|R_{n=2}(0)|^2}{2\pi} = 4.5 \text{ GeV}^3, \\
\langle \mathcal{O}(b\bar{b}([{}^3P_0]_1) \rightarrow \chi_{b0}(2P)) \rangle &= 3N_c \frac{|R'_{n=2}(0)|^2}{2\pi} = 0.036m_{\text{bottom}}^2 \text{ GeV}^3, \\
\langle \mathcal{O}(b\bar{b}([{}^3S_1]_1) \rightarrow \Upsilon(3S)) \rangle &= 3N_c \frac{|R_{n=3}(0)|^2}{2\pi} = 4.3 \text{ GeV}^3,
\end{aligned} \tag{16}$$

where we use  $m_{\text{bottom}} = 4.88\text{GeV}$  [13, 14].

## 2. Color Octet Matrix elements

The color-octet operators can not be related to the non-relativistic wavefunctions of  $Q\bar{Q}$  since it involves a higher Fock state. We used following values for Color Octet Matrix



elements as given in Ref. [17].

$$\begin{aligned}
\langle \mathcal{O}(c\bar{c}([{}^3S_1]_8) \rightarrow J/\psi) \rangle &= (0.0013 \pm 0.0013) \text{ GeV}^3, \\
\langle \mathcal{O}(c\bar{c}([{}^1S_0]_8) \rightarrow J/\psi) \rangle &= (0.018 \pm 0.0087) \text{ GeV}^3, \\
&= \langle \mathcal{O}(c\bar{c}([{}^3P_0]_8) \rightarrow J/\psi) \rangle / (m_{\text{charm}}^2), \\
\langle \mathcal{O}(c\bar{c}([{}^3S_1]_8) \rightarrow \psi(2S)) \rangle &= (0.0033 \pm 0.00021) \text{ GeV}^3, \\
\langle \mathcal{O}(c\bar{c}([{}^1S_0]_8) \rightarrow \psi(2S)) \rangle &= (0.0080 \pm 0.00067) \text{ GeV}^3, \\
&= \langle \mathcal{O}(c\bar{c}([{}^3P_0]_8) \rightarrow J/\psi) \rangle / (m_{\text{charm}}^2), \\
\langle \mathcal{O}(c\bar{c}([{}^3P_1]_8) \rightarrow J/\psi) \rangle &= 3 \times \langle \mathcal{O}(c\bar{c}([{}^3P_0]_8) \rightarrow J/\psi) \rangle, \\
\langle \mathcal{O}(c\bar{c}([{}^3P_2]_8) \rightarrow J/\psi) \rangle &= 5 \times \langle \mathcal{O}(c\bar{c}([{}^3P_0]_8) \rightarrow J/\psi) \rangle, \\
\langle \mathcal{O}(c\bar{c}([{}^3S_1]_8) \rightarrow \chi_{c0}(1P)) \rangle &= (0.00187 \pm 0.00025) \text{ GeV}^3,
\end{aligned} \tag{17}$$

Since the shape of the short distance part as a function of  $p_T$  is very similar for  $[{}^1S_0]_8$  and  $[{}^3P_0]_8$  contributions [13, 14], only fit a linear combination of these elements is fitted.

The octet matrix elements for the bottomonia are obtained by fitting TeVatron [18] and the LHC [19] data and are as follows:

$$\begin{aligned}
\langle \mathcal{O}(b\bar{b}([{}^3S_1]_8) \rightarrow \Upsilon(1S)) \rangle &= (0.0477 \pm 0.0334) \text{ GeV}^3, \\
\langle \mathcal{O}(b\bar{b}([{}^1S_0]_8) \rightarrow \Upsilon(1S)) \rangle &= (0.0121 \pm 0.040) \text{ GeV}^3, \\
&= \langle \mathcal{O}(b\bar{b}([{}^3P_0]_8) \rightarrow \Upsilon(1S)) \rangle / (5m_{\text{bottom}}^2), \\
\langle \mathcal{O}(b\bar{b}([{}^3S_1]_8) \rightarrow \chi_{b0}(1P)) \rangle &= (0.1008) \text{ GeV}^3, \\
\langle \mathcal{O}(b\bar{b}([{}^3S_1]_8) \rightarrow \Upsilon(2S)) \rangle &= (0.0224 \pm 0.02) \text{ GeV}^3, \\
\langle \mathcal{O}(b\bar{b}([{}^1S_0]_8) \rightarrow \Upsilon(2S)) \rangle &= (-0.0067 \pm 0.0084) \text{ GeV}^3, \\
&= \langle \mathcal{O}(b\bar{b}([{}^3P_0]_8) \rightarrow \Upsilon(2S)) \rangle / (5m_{\text{bottom}}^2), \\
\langle \mathcal{O}(b\bar{b}([{}^3S_1]_8) \rightarrow \chi_{b0}(2P)) \rangle &= (0.0324) \text{ GeV}^3, \\
\langle \mathcal{O}(b\bar{b}([{}^3S_1]_8) \rightarrow \Upsilon(3S)) \rangle &= (0.0513 \pm 0.0085) \text{ GeV}^3, \\
\langle \mathcal{O}(b\bar{b}([{}^1S_0]_8) \rightarrow \Upsilon(3S)) \rangle &= (0.0002 \pm 0.0062) \text{ GeV}^3, \\
&= \langle \mathcal{O}(b\bar{b}([{}^3P_0]_8) \rightarrow \Upsilon(3S)) \rangle / (5m_{\text{bottom}}^2)
\end{aligned} \tag{18}$$

For a more sophisticated fitting of the color-octet matrix elements including NLO effects, see [20–22].

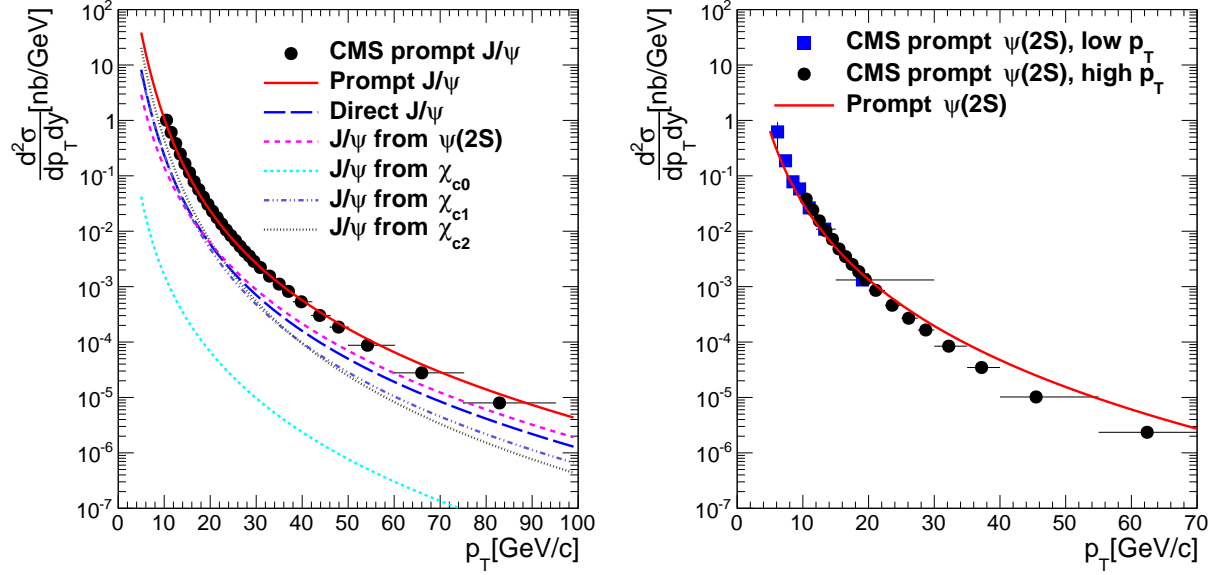


FIG. 1. (Color online) Differential production cross-section of  $J/\psi$  and  $\psi(2S)$  as a function of  $p_T$  compared with the CMS [8, 9] data.

### III. RESULT AND DISCUSSION

Figure 1 (a) shows the differential production cross-section of prompt  $J/\psi$  as a function of transverse momentum ( $p_T$ ) compared with the CMS measurements [9]. We have calculated differential production cross-sections for all the relevant resonances. These cross sections are then appropriately scaled with proper branching fractions and total cross section for prompt  $J/\psi$  is calculated and shown in Fig. 1 (a). The  $\psi(2S)$  has largest contribution at high  $p_T$  while at low  $p_T$  contribution from  $\chi_{c1}$  and  $\chi_{c2}$  exceed the  $\psi(2S)$  contribution. After adding all the contributions, the  $p_T$  dependence of prompt  $J/\psi$  differential production cross-section are described reasonably well by our calculations. The  $\psi(2S)$  has no significant feed-down contributions from higher mass states. We call this direct contribution as "prompt  $\psi(2S)$ " to be consistent with the  $J/\psi$  calculations. Figure 1(b) shows the differential production cross-section of prompt  $\psi(2S)$  as a function of  $p_T$  compared with the CMS measurements [9]. Here also our calculations qualitatively reproduced the measured cross section.

#### IV. SUMMARY

We have calculated the differential production cross-section of prompt  $J/\psi$  and prompt  $\psi(2S)$  as a function of transverse momentum. For the  $J/\psi$  meson all the relevant contributions from higher mass states are estimated. The  $\psi(2S)$  meson does not have significant contributions from higher mass states. The calculations for prompt  $J/\psi$  and prompt  $\psi(2S)$  are compared with the measured data at LHC. A fairly good agreement between measured data and calculations is observed in low  $p_T$  range. The reevaluation of LDME is in progress using latest data from LHC to achieve good description of data in the whole  $p_T$  range.

## Appendix A: Short distance pQCD cross sections for quarkonia production

Here we list the lowest order QCD cross sections for the resonance production used in our calculations. We write the formulas in terms of the invariants  $\hat{s}, \hat{t}, \hat{u}$ . where  $\hat{s}^2 + \hat{t}^2 + \hat{u}^2 = M^2$  and  $M$  is the mass of the resonance considered. These parton level invariants are related with the rapidity,  $y$  and transeverse momentum  $p_T$  of the resonance with following relations

$$\begin{aligned}\hat{s} &= x_a x_b s \\ \hat{t} &= M^2 - x_a \sqrt{s} m_T e^{-y} \\ \hat{u} &= M^2 - x_b \sqrt{s} m_T e^y\end{aligned}\tag{A1}$$

The subprocesses of resonance production can be grouped as follows.

To order  $\alpha_s^2$  one only has the gluon fusion processes,  $g g \rightarrow^{(2S+1)} L_J$ . This process gives resonance with very small  $p_T$ , so we do not use these corss sections in our calculations.

To order  $\alpha_s^3$ , on the other hand, one has typically two-by-two scattering processes. The relevant cross sections are given below:

### a. Color Singlet PQCD cross sections

- $g q \rightarrow^{(2S+1)} L_J q$  or  $(q \rightarrow \bar{q})$

$$\begin{aligned}\frac{d\sigma}{d\hat{t}}(^1S_0) &= \frac{2\pi\alpha_s^3(R_0)^2}{9M\hat{s}^2} \cdot \frac{(\hat{t} - M^2)^2 - 2\hat{s}\hat{u}}{(-\hat{t})(\hat{t} - M^2)^2} \\ \frac{d\sigma}{d\hat{t}}(^3P_0) &= \frac{8\pi\alpha_s^3(R'_1)^2}{9M^3\hat{s}^2} \cdot \frac{(\hat{t} - 3M^2)^2(\hat{s}^2 + \hat{u}^2)}{(-\hat{t})(\hat{t} - M^2)^4} \\ \frac{d\sigma}{d\hat{t}}(^3P_1) &= \frac{16\pi\alpha_s^3(R'_1)^2}{3M^3\hat{s}^2} \cdot \frac{-\hat{t}(\hat{s}^2 + \hat{u}^2) - 4M^2\hat{s}\hat{u}}{(\hat{t} - M^2)^4} \\ \frac{d\sigma}{d\hat{t}}(^3P_2) &= \frac{16\pi\alpha_s^3(R'_1)^2}{9M^3\hat{s}^2} \cdot \frac{(\hat{t} - M^2)^2(\hat{t}^2 + 6M^4) - 2\hat{s}\hat{u}(\hat{t}^2 - 6M^2(\hat{t} - M^2))}{(-\hat{t})(\hat{t} - M^2)^4}\end{aligned}\tag{A2}$$

- $q \bar{q} \rightarrow^{(2S+1)} L_J g$

$$\frac{d\sigma}{d\hat{t}}(^{(2S+1)} L_J) = -\frac{8}{3} \frac{\hat{t}^2}{\hat{s}^2} \frac{d\sigma}{d\hat{t}}(gq \rightarrow^{(2S+1)} L_J q)|_{\hat{t} \leftrightarrow \hat{u}}\tag{A3}$$

- $g g \rightarrow {}^{(2S+1)}L_J g$

$$\begin{aligned}
\frac{d\sigma}{d\hat{t}}({}^3S_1) &= \frac{5\pi\alpha_s^3(R_0)^2}{9M\hat{s}^2} \cdot \frac{M^2}{(\hat{s}-M^2)^2(\hat{t}-M^2)^2(\hat{u}-M^2)^2} \\
&\quad \cdot \{[\hat{s}^2(\hat{s}-M^2)^2] + [\hat{s} \rightarrow \hat{t}] + [\hat{s} \rightarrow \hat{u}]\} \\
\frac{d\sigma}{d\hat{t}}({}^1S_0) &= \frac{\pi\alpha_s^3(R_0)^2}{2M\hat{s}^2} \frac{1}{\hat{s}\hat{t}\hat{u}(\hat{s}-M^2)^2(\hat{t}-M^2)^2(\hat{u}-M^2)^2} \\
&\quad \cdot \{[\hat{s}^4(\hat{s}-M^2)^2((\hat{s}-M^2)^2+2M^4) \\
&\quad - \frac{4}{3}\hat{s}\hat{t}\hat{u}(\hat{s}^2+\hat{t}^2+\hat{u}^2)(\hat{s}-M^2)(\hat{t}-M^2)(\hat{u}-M^2) \\
&\quad + \frac{16}{3}M^2\hat{s}\hat{t}\hat{u}(\hat{s}^2\hat{t}^2+\hat{s}^2\hat{u}^2+\hat{t}^2\hat{u}^2) \\
&\quad + \frac{28}{3}M^4\hat{s}^2\hat{t}^2\hat{u}^2] + [\hat{s} \leftrightarrow \hat{t}] + [\hat{s} \leftrightarrow \hat{u}]\}
\end{aligned} \tag{A4}$$

We define two new variables as a combination of  $\hat{s}, \hat{t}$  and  $\hat{u}$ . These variables can be used to define the  $g g \rightarrow {}^{(2S+1)}L_J g$  cross sections.

$$\begin{aligned}
P &= \hat{s}\hat{t} + \hat{t}\hat{u} + \hat{u}\hat{s} \\
Q &= \hat{s}\hat{t}\hat{u}
\end{aligned} \tag{A5}$$

$$\begin{aligned}
\frac{d\sigma}{d\hat{t}}(^1S_0) &= \frac{\pi\alpha_s^3(R_0)^2}{M\hat{s}^2} \frac{P^2(M^8 - 2M^4P + P^2 + 2M^2Q)}{Q(Q - M^2P)^2} \\
\frac{d\sigma}{d\hat{t}}(^3S_1) &= \frac{10\pi\alpha_s^3(R_0)^2}{9\hat{s}^2} \frac{M(P^2 - M^2Q)}{(Q - M^2P)^2} \\
\frac{d\sigma}{d\hat{t}}(^1P_1) &= \frac{40\pi\alpha_s^3(R'_1)^2}{3M\hat{s}^2} \frac{[-M^{10}P + M^6P^2 + Q(5M^8 - 7M^4P + 2P^2) + 4M^2Q^2]}{(Q - M^2P)^3} \\
\frac{d\sigma}{d\hat{t}}(^3P_0) &= \frac{4\pi\alpha_s^3(R'_1)^2}{M^3\hat{s}^2} \frac{1}{Q(Q - M^2P)^4} [9M^4P^4(M^8 - 2M^4P + P^2) \\
&\quad - 6M^2P^3Q(2M^8 - 5M^4P + P^2) \\
&\quad - P^2Q^2(M^8 + 2M^4P - P^2) \\
&\quad + 2M^2PQ^3(M^4 - P) + 6M^4Q^4] \\
\frac{d\sigma}{d\hat{t}}(^3P_1) &= \frac{12\pi\alpha_s^3(R'_1)^2}{M^3\hat{s}^2} \frac{P^2\{M^2P^2(M^4 - 4P) - 2Q(M^8 - 5M^4P - P^2) - 15M^2Q^2\}}{(Q - M^2P)^4} \\
\frac{d\sigma}{d\hat{t}}(^3P_2) &= \frac{4\pi\alpha_s^3(R'_1)^2}{M^3\hat{s}^2} \frac{1}{Q(Q - M^2P)^4} \\
&\quad \{12M^4P^4(M^8 - 2M^4P + P^2) - 3M^2P^3Q(8M^8 - M^4P + 4P^2) \\
&\quad - 2P^2Q^2(7M^8 - 43M^4P - P^2) + M^2PQ^3(16M^4 - 61P) \\
&\quad + 12M^4Q^4\}
\end{aligned} \tag{A6}$$

*b. Color Octet PQCD cross sections*

We list below short distance squared amplitudes for  $2 \rightarrow 2$  scattering processes which mediate color-octet quarkonia production. These expressions are averaged over initial spins and colors of the two incident partons. The helicity levels of outgoing  $J = 1$  and  $J = 2$  pairs are labeled by the subscript  $h$ . The total squared amplitudes for creating specific quarkonia states can be obtained by multiplying these process-independent short distance expressions with appropriate long distance NRQCD matrix elements.

- $q \bar{q} \rightarrow Q\bar{Q}^{[(2S+1)L_J^{(8)}]} g$

$$\begin{aligned}
\sum_{|h|=0}^{\infty} |\mathcal{A}(q\bar{q} \rightarrow Q\bar{Q}[{}^1S_0^{(8)}]g)|^2 &= \frac{5(4\pi\alpha_s)^3}{27M^3} \frac{\hat{t}^2 + \hat{u}^2}{\hat{s}(\hat{s} - M^2)^2} \\
\sum_{|h|=0}^{\infty} |\mathcal{A}(q\bar{q} \rightarrow Q\bar{Q}[{}^3S_1^{(8)}]g)|^2 &= \frac{8(4\pi\alpha_s)^3}{81M^3} \frac{M^2\hat{s}}{(\hat{s} - M^2)^4} [4(\hat{t}^2 + \hat{u}^2) - \hat{t}\hat{u}] \\
\sum_{|h|=1}^{\infty} |\mathcal{A}(q\bar{q} \rightarrow Q\bar{Q}[{}^3S_1^{(8)}]g)|^2 &= \frac{2(4\pi\alpha_s)^3}{81M^3} \frac{\hat{s}^2 + M^4}{(\hat{s} - M^2)^4} \frac{\hat{t}^2 + \hat{u}^2}{\hat{t}\hat{u}} [4(\hat{t}^2 + \hat{u}^2) - \hat{t}\hat{u}] \\
\sum_{|h|=0}^{\infty} |\mathcal{A}(q\bar{q} \rightarrow Q\bar{Q}[{}^3P_0^{(8)}]g)|^2 &= \frac{20(4\pi\alpha_s)^3}{81M^3} \frac{(\hat{s} - 3M^2)^2(\hat{t}^2 + \hat{u}^2)}{\hat{s}(\hat{s} - M^2)^4} \\
\sum_{|h|=0}^{\infty} |\mathcal{A}(q\bar{q} \rightarrow Q\bar{Q}[{}^3P_1^{(8)}]g)|^2 &= \frac{40(4\pi\alpha_s)^3}{81M^3} \frac{\hat{s}(\hat{t}^2 + \hat{u}^2)}{(\hat{s} - M^2)^4} \\
\sum_{|h|=1}^{\infty} |\mathcal{A}(q\bar{q} \rightarrow Q\bar{Q}[{}^3P_1^{(8)}]g)|^2 &= \frac{160(4\pi\alpha_s)^3}{81M^3} \frac{M^2\hat{t}\hat{u}}{(\hat{s} - M^2)^4} \\
\sum_{|h|=0}^{\infty} |\mathcal{A}(q\bar{q} \rightarrow Q\bar{Q}[{}^3P_2^{(8)}]g)|^2 &= \frac{8(4\pi\alpha_s)^3}{81M^3} \frac{\hat{s}(\hat{t}^2 + \hat{u}^2)}{(\hat{s} - M^2)^4} \\
\sum_{|h|=1}^{\infty} |\mathcal{A}(q\bar{q} \rightarrow Q\bar{Q}[{}^3P_2^{(8)}]g)|^2 &= \frac{32(4\pi\alpha_s)^3}{27M^3} \frac{M^2\hat{t}\hat{u}}{(\hat{s} - M^2)^4} \\
\sum_{|h|=2}^{\infty} |\mathcal{A}(q\bar{q} \rightarrow Q\bar{Q}[{}^3P_2^{(8)}]g)|^2 &= \frac{16(4\pi\alpha_s)^3}{27M^3} \frac{M^4(\hat{t}^2 + \hat{u}^2)}{\hat{s}(\hat{s} - M^2)^4}
\end{aligned} \tag{A7}$$

- $g \ q \rightarrow Q\bar{Q}[{}^{(2S+1)}L_J^{(8)}] \ q$

$$\begin{aligned}
\sum_{|h|=0}^{\infty} |\mathcal{A}(gq \rightarrow Q\bar{Q}[^1S_0^{(8)}]q)|^2 &= -\frac{5(4\pi\alpha_s)^3}{72M} \frac{\hat{s}^2 + \hat{u}^2}{\hat{t}(\hat{t} - M^2)^2} \\
\sum_{h=0}^{\infty} |\mathcal{A}(gq \rightarrow Q\bar{Q}[^3S_1^{(8)}]q)|^2 &= -\frac{(4\pi\alpha_s)^3}{54M^3} \frac{M^2\hat{t}[4(\hat{s}^2 + \hat{u}^2) - \hat{s}\hat{u}]}{[(\hat{s} - M^2)(\hat{t} - M^2)]^2} \\
\sum_{|h|=1}^{\infty} |\mathcal{A}(gq \rightarrow Q\bar{Q}[^3S_1^{(8)}]q)|^2 &= -\frac{(4\pi\alpha_s)^3}{108M^3} \\
&\quad \times \frac{(\hat{s}^2 + \hat{u}^2 + 2M^2\hat{t})(\hat{s} - M^2)^2 - 2M^2\hat{s}\hat{t}\hat{u}}{\hat{s}\hat{u}[(\hat{s} - M^2)(\hat{t} - M^2)]^2} \\
&\quad \times [4(\hat{s}^2 + \hat{u}^2) - \hat{s}\hat{u}] \\
\sum_{|h|=0}^{\infty} |\mathcal{A}(gq \rightarrow Q\bar{Q}[^3P_0^{(8)}]q)|^2 &= -\frac{5(4\pi\alpha_s)^3}{54M^3} \frac{(\hat{t} - 3M^2)^2(\hat{s}^2 + \hat{u}^2)}{\hat{t}(\hat{t} - M^2)^4} \\
\sum_{h=0}^{\infty} |\mathcal{A}(gq \rightarrow Q\bar{Q}[^3P_1^{(8)}]q)|^2 &= -\frac{5(4\pi\alpha_s)^3}{27M^3} \frac{\hat{t}[\hat{s}^2(\hat{s} - M^2)^2 + \hat{u}^2(\hat{s} + M^2)^2]}{(\hat{t} - M^2)^4(\hat{s} - M^2)^2} \\
\sum_{|h|=1}^{\infty} |\mathcal{A}(gq \rightarrow Q\bar{Q}[^3P_1^{(8)}]q)|^2 &= -\frac{20(4\pi\alpha_s)^3}{27M^3} \frac{M^2\hat{s}\hat{u}(\hat{t}^2 + \hat{t}\hat{u} + \hat{u}^2)}{(\hat{t} - M^2)^4(\hat{s} - M^2)^2} \tag{A8} \\
\sum_{h=0}^{\infty} |\mathcal{A}(gq \rightarrow Q\bar{Q}[^3P_2^{(8)}]q)|^2 &= -\frac{(4\pi\alpha_s)^3}{27M^3} \frac{\hat{t}}{(\hat{t} - M^2)^4} \\
&\quad \times [\hat{s}^2 + \hat{u}^2 + 12M^2\hat{s}\hat{u}^2 \frac{\hat{s}^2 + M^2\hat{s} + M^4}{(\hat{s} - M^2)^4}] \\
\sum_{|h|=1}^{\infty} |\mathcal{A}(gq \rightarrow Q\bar{Q}[^3P_2^{(8)}]q)|^2 &= -\frac{4(4\pi\alpha_s)^3}{9M^3} \frac{M^2\hat{s}\hat{u}}{(\hat{t} - M^2)^4} \\
&\quad \times \frac{(\hat{s} - M^2)^2(\hat{s}^2 + M^4) - (\hat{s} + M^2)^2\hat{t}\hat{u}}{(\hat{s} - M^2)^4} \\
\sum_{|h|=2}^{\infty} |\mathcal{A}(gq \rightarrow Q\bar{Q}[^3P_2^{(8)}]q)|^2 &= -\frac{2(4\pi\alpha_s)^3}{9M^3} \frac{M^4}{\hat{t}(\hat{t} - M^2)^4} \\
&\quad \times [\hat{s}^2 + \hat{u}^2 + 2\hat{s}^2\hat{t}\hat{u} \frac{(\hat{s} - M^2)(2\hat{t} + \hat{u}) - \hat{u}^2}{(\hat{s} - M^2)^4}]
\end{aligned}$$

- $g g \rightarrow Q\bar{Q}[^{(2S+1)}L_J^{(8)}] g$  ( The  $gg \rightarrow Q\bar{Q}[^3P_J^{(8)}] g$  squared amplitudes are expressed in terms of the variables  $\hat{s}$  and  $\hat{z} \equiv \sqrt{\hat{t}\hat{u}}$ .)



$$\begin{aligned}
\sum_{\bar{h}} |\mathcal{A}(gg \rightarrow Q\bar{Q}[^1S_0^{(8)}]g)|^2 &= \frac{5(4\pi\alpha_s)^3}{16M} [\hat{s}^2(\hat{s} - M^2)^2 + \hat{s}\hat{t}\hat{u}(M^2 - 2\hat{s}) + (\hat{t}\hat{u})^2] \\
&\quad \times \frac{(\hat{s}^2 - M^2\hat{s} + M^4)^2 - \hat{t}\hat{u}(2\hat{t}^2 + 3\hat{t}\hat{u} + 2\hat{u}^2)}{\hat{s}\hat{t}\hat{u}[(\hat{s} - M^2)(\hat{t} - M^2)(\hat{u} - M^2)]^2} \\
\sum_{h=0} |\mathcal{A}(gg \rightarrow Q\bar{Q}[^3S_1^{(8)}]g)|^2 &= -\frac{(4\pi\alpha_s)^3}{144M^3} \frac{2M^2\hat{s}}{(\hat{s} - M^2)^2} (\hat{t}^2 + \hat{u}^2)\hat{t}\hat{u} \\
&\quad \times \frac{27(\hat{s}\hat{t} + \hat{t}\hat{u} + \hat{u}\hat{s}) - 19M^4}{[(\hat{s} - M^2)(\hat{t} - M^2)(\hat{u} - M^2)]^2} \\
\sum_{|h|=1} |\mathcal{A}(gg \rightarrow Q\bar{Q}[^3S_1^{(8)}]g)|^2 &= -\frac{(4\pi\alpha_s)^3}{144M^3} \frac{\hat{s}^2}{(\hat{s} - M^2)^2} \\
&\quad \times [(\hat{s} - M^2)^4 + \hat{t}^4 + \hat{u}^4 + 2M^4\left(\frac{\hat{t}\hat{u}}{\hat{s}}\right)^2] \\
&\quad \times \frac{27(\hat{s}\hat{t} + \hat{t}\hat{u} + \hat{u}\hat{s}) - 19M^4}{[(\hat{s} - M^2)(\hat{t} - M^2)(\hat{u} - M^2)]^2} \\
\sum_{\bar{h}} |\mathcal{A}(gg \rightarrow Q\bar{Q}[^3P_0^{(8)}]g)|^2 &= \frac{5(4\pi\alpha_s)^3}{12M^3} \frac{1}{[\hat{s}\hat{z}^2(\hat{s} - M^2)^4(\hat{s}M^2 + \hat{z}^2)^4]} \\
&\quad \times \left\{ \hat{s}^2\hat{z}^4(\hat{s}^2 - \hat{z}^2)^4 + M^2\hat{s}\hat{z}^2(\hat{s}^2 - \hat{z}^2)^2(3\hat{s}^2 - 2\hat{z}^2)(2\hat{s}^4 - 6\hat{s}^2\hat{z}^2 + 3\hat{z}^4) \right. \\
&\quad + M^4[9\hat{s}^{12} - 84\hat{s}^{10}\hat{z}^2 + 265\hat{s}^8\hat{z}^4 - 382\hat{s}^6\hat{z}^6 + 276\hat{s}^4\hat{z}^8 - 88\hat{s}^2\hat{z}^{10} + 9\hat{z}^{12}] \\
&\quad - M^6\hat{s}[54\hat{s}^{10} - 357\hat{s}^8\hat{z}^2 + 844\hat{s}^6\hat{z}^4 - 898\hat{s}^4\hat{z}^6 + 439\hat{s}^2\hat{z}^8 - 81\hat{z}^{10}] \\
&\quad + M^8[153\hat{s}^{10} - 798\hat{s}^8\hat{z}^2 + 1415\hat{s}^6\hat{z}^4 - 1041\hat{s}^4\hat{z}^6 + 301\hat{s}^2\hat{z}^8 - 18\hat{z}^{10}] \\
&\quad - M^{10}\hat{s}[270\hat{s}^8 - 1089\hat{s}^6\hat{z}^2 + 1365\hat{s}^4\hat{z}^4 - 616\hat{s}^2\hat{z}^6 + 87\hat{z}^8] \\
&\quad + M^{12}[324\hat{s}^8 - 951\hat{s}^6\hat{z}^2 + 769\hat{s}^4\hat{z}^4 - 189\hat{s}^2\hat{z}^6 + 9\hat{z}^8] \\
&\quad - 9M^{14}\hat{s}[(6\hat{s}^2 - \hat{z}^2)(5\hat{s}^4 - 9\hat{s}^2\hat{z}^2 + 3\hat{z}^4)] \\
&\quad + 3M^{16}\hat{s}^2[51\hat{s}^4 - 59\hat{s}^2\hat{z}^2 + 12\hat{z}^4] \\
&\quad - 27M^{18}\hat{s}^3[2\hat{s}^2 - \hat{z}^2] \\
&\quad \left. + 9M^{20}\hat{s}^4 \right\}
\end{aligned}$$

(A9)

$$\begin{aligned}
\sum_{h=0}^{\infty} |\mathcal{A}(gg \rightarrow Q\bar{Q}[{}^3P_1^{(8)}]g)|^2 &= \frac{5(4\pi\alpha_s)^3}{6M^3} \frac{1}{[(\hat{s} - M^2)^4(\hat{s}M^2 + \hat{z}^2)^4]} \\
&\quad \times \hat{s}\hat{z}^2 [(\hat{s}^2 - \hat{z}^2)^2 - 2M^2\hat{s}\hat{z}^2 - M^4(\hat{s}^2 + 2\hat{z}^2) + M^8] \\
&\quad \times [(\hat{s}^2 - \hat{z}^2)^2 - M^2\hat{s}(2\hat{s}^2 - \hat{z}^2) + M^4\hat{s}^2] \\
\sum_{|h|=1}^{\infty} |\mathcal{A}(gg \rightarrow Q\bar{Q}[{}^3P_1^{(8)}]g)|^2 &= \frac{5(4\pi\alpha_s)^3}{6M^3} \frac{1}{[(\hat{s} - M^2)^4(\hat{s}M^2 + \hat{z}^2)^4]} \\
&\quad \times M^2 \left\{ 2(\hat{s}^2 - \hat{z}^2)^2(\hat{s}^6 - 4\hat{s}^4\hat{z}^2 + \hat{s}^2\hat{z}^4 - \hat{z}^6) \right. \\
&\quad - M^2\hat{s}(2\hat{s}^2 - \hat{z}^2)(5\hat{s}^6 - 17\hat{s}^4\hat{z}^2 + 9\hat{s}^2\hat{z}^4 - \hat{z}^6) \\
&\quad + M^4(21\hat{s}^8 - 49\hat{s}^6\hat{z}^2 + 21\hat{s}^4\hat{z}^4 - 4\hat{s}^2\hat{z}^6 + \hat{z}^8) \\
&\quad - M^6\hat{s}(24\hat{s}^6 - 30\hat{s}^4\hat{z}^2 + 6\hat{s}^2\hat{z}^4 - \hat{z}^6) \\
&\quad + M^8\hat{s}^2(16\hat{s}^4 - 9\hat{s}^2\hat{z}^2 + 2\hat{z}^4) \\
&\quad - M^{10}\hat{s}^3(6\hat{s}^2 - \hat{z}^2) \\
&\quad \left. + M^{12}\hat{s}^4 \right\} \\
\sum_{h=0}^{\infty} |\mathcal{A}(gg \rightarrow Q\bar{Q}[{}^3P_2^{(8)}]g)|^2 &= \frac{(4\pi\alpha_s)^3}{6M^3} \frac{\hat{s}\hat{z}^2}{[(\hat{s} - M^2)^6(\hat{s}M^2 + \hat{z}^2)^4]} \\
&\quad \left\{ \hat{s}^2(\hat{s}^2 - \hat{z}^2)^4 - M^2\hat{s}\hat{z}^2(\hat{s}^2 - \hat{z}^2)^2(11\hat{s}^2 + 2\hat{z}^2) \right. \\
&\quad + M^4[\hat{s}^8 - 12\hat{s}^6\hat{z}^2 + 41\hat{s}^4\hat{z}^4 - 20\hat{s}^2\hat{z}^6 + \hat{z}^8] \\
&\quad - M^6\hat{s}[4\hat{s}^6 - 26\hat{s}^4\hat{z}^2 - \hat{s}^2\hat{z}^4 - 5\hat{z}^6] \\
&\quad + M^8[29\hat{s}^6 - 114\hat{s}^4\hat{z}^2 + 108\hat{s}^2\hat{z}^4 - 10\hat{z}^6] \\
&\quad - M^{10}\hat{s}[65\hat{s}^4 - 104\hat{s}^2\hat{z}^2 - 33\hat{z}^4] \\
&\quad + M^{12}[54\hat{s}^4 - 20\hat{s}^2\hat{z}^2 + 7\hat{z}^4] \\
&\quad - M^{14}\hat{s}[23\hat{s}^2 + 5\hat{z}^2] \\
&\quad \left. + 7M^{16}\hat{s}^2 \right\}
\end{aligned} \tag{A10}$$

$$\begin{aligned}
\sum_{|h|=1}^{\bar{}} |\mathcal{A}(gg \rightarrow Q\bar{Q}[{}^3P_2^{(8)}]g)|^2 &= \frac{(4\pi\alpha_s)^3}{2M^3} \frac{M^2}{[(\hat{s} - M^2)^6(\hat{s}M^2 + \hat{z}^2)^4]} \\
&\times \left\{ 2\hat{s}^2(\hat{s}^2 - \hat{z}^2)^2(\hat{s}^6 - 4\hat{s}^4\hat{z}^2 + \hat{s}^2\hat{z}^4 - \hat{z}^6) \right. \\
&- M^2\hat{s}[10\hat{s}^{10} - 37\hat{s}^8\hat{z}^2 + 19\hat{s}^6\hat{z}^4 + 11\hat{s}^4\hat{z}^6 - \hat{s}^2\hat{z}^8 - 4\hat{z}^{10}] \\
&+ M^4[25\hat{s}^{10} - 61\hat{s}^8\hat{z}^2 + 27\hat{s}^6\hat{z}^4 - 34\hat{s}^4\hat{z}^6 + 23\hat{s}^2\hat{z}^8 - 2\hat{z}^{10}] \\
&- M^6\hat{s}[42\hat{s}^8 - 77\hat{s}^6\hat{z}^2 + 41\hat{s}^4\hat{z}^4 - 22\hat{s}^2\hat{z}^6 + 17\hat{z}^8] \\
&+ M^8[53\hat{s}^8 - 88\hat{s}^6\hat{z}^2 + 69\hat{s}^4\hat{z}^4 - 68\hat{s}^2\hat{z}^6 + 3\hat{z}^8] \\
&- M^{10}\hat{s}[54\hat{s}^6 - 85\hat{s}^4\hat{z}^2 + 60\hat{s}^2\hat{z}^4 - 9\hat{z}^6] \\
&+ M^{12}\hat{s}^2[43\hat{s}^4 - 47\hat{s}^2\hat{z}^2 + 20\hat{z}^4] \\
&- M^{14}\hat{s}^3[22\hat{s}^2 - 9\hat{z}^2] \\
&\left. + 5M^{16}\hat{s}^4 \right\} \\
\sum_{|h|=2}^{\bar{}} |\mathcal{A}(gg \rightarrow Q\bar{Q}[{}^3P_2^{(8)}]g)|^2 &= \frac{(4\pi\alpha_s)^3}{2M^3} \frac{M^4}{[\hat{s}\hat{z}^2(\hat{s} - M^2)^6(\hat{s}M^2 + \hat{z}^2)^4]} \\
&\times \left\{ 2\hat{s}^2[\hat{s}^{12} - 8\hat{s}^{10}\hat{z}^2 + 22\hat{s}^8\hat{z}^4 - 24\hat{s}^6\hat{z}^6 + 10\hat{s}^4\hat{z}^8 - 3\hat{s}^2\hat{z}^{10} + \hat{z}^{12}] \right. \\
&- M^2\hat{s}[16\hat{s}^{12} - 102\hat{s}^{10}\hat{z}^2 + 210\hat{s}^8\hat{z}^4 - 153\hat{s}^6\hat{z}^6 + 36\hat{s}^4\hat{z}^8 - 6\hat{s}^2\hat{z}^{10} + 4\hat{z}^{12}] \\
&+ M^4[60\hat{s}^{12} - 306\hat{s}^{10}\hat{z}^2 + 482\hat{s}^8\hat{z}^4 - 271\hat{s}^6\hat{z}^6 + 77\hat{s}^4\hat{z}^8 - 18\hat{s}^2\hat{z}^{10} + 2\hat{z}^{12}] \\
&- M^6\hat{s}[140\hat{s}^{10} - 573\hat{s}^8\hat{z}^2 + 710\hat{s}^6\hat{z}^4 - 344\hat{s}^4\hat{z}^6 + 91\hat{s}^2\hat{z}^8 - 18\hat{z}^{10}] \\
&+ M^8[226\hat{s}^{10} - 741\hat{s}^8\hat{z}^2 + 737\hat{s}^6\hat{z}^4 - 310\hat{s}^4\hat{z}^6 + 77\hat{s}^2\hat{z}^8 - 4\hat{z}^{10}] \\
&- M^{10}\hat{s}[264\hat{s}^8 - 686\hat{s}^6\hat{z}^2 + 541\hat{s}^4\hat{z}^4 - 177\hat{s}^2\hat{z}^6 + 25\hat{z}^8] \\
&+ M^{12}[226\hat{s}^8 - 452\hat{s}^6\hat{z}^2 + 261\hat{s}^4\hat{z}^4 - 55\hat{s}^2\hat{z}^6 + 2\hat{z}^8] \\
&- M^{14}\hat{s}[140\hat{s}^6 - 201\hat{s}^4\hat{z}^2 + 71\hat{s}^2\hat{z}^4 - 6\hat{z}^6] \\
&+ M^{16}\hat{s}^2[60\hat{s}^4 - 53\hat{s}^2\hat{z}^2 + 8\hat{z}^4] \\
&- 2M^{18}\hat{s}^3[8\hat{s}^2 - 3\hat{z}^2] \\
&\left. + 2M^{20}\hat{s}^4 \right\}
\end{aligned} \tag{A11}$$

- 
- [1] T. Matsui and H. Satz, “ $J/\psi$  Suppression by Quark-Gluon Plasma Formation”, Phys. Lett. B **178**, 416 (1986).
  - [2] J. Schukraft, “Heavy Ion Physics at the LHC: What’s new ? What’s next ?”, arXiv:1311.1429 [hep-ex].
  - [3] L. Kluberg and H. Satz, “Color Deconfinement and Charmonium Production in Nuclear Collisions,” arXiv:0901.3831 [hep-ph].
  - [4] N. Brambilla, S. Eidelman, B. K. Heltsley, R. Vogt, G. T. Bodwin, E. Eichten, A. D. Frawley and A. B. Meyer *et al.*, “Heavy quarkonium: progress, puzzles, and opportunities,” Eur. Phys. J. C **71**, 1534 (2011).
  - [5] A. Adare *et al.* [PHENIX Collaboration], “ $J/\psi$  suppression at forward rapidity in Au+Au collisions at  $\sqrt{s_{NN}} = 200$  GeV,” Phys. Rev. C **84**, 054912 (2011).
  - [6] A. Andronic, P. Braun-Munzinger, K. Redlich and J. Stachel, “Statistical hadronization of charm in heavy ion collisions at SPS, RHIC and LHC,” Phys. Lett. B **571**, 36 (2003).
  - [7] H. L. Lai, M. Guzzi, J. Huston, Z. Li, P. M. Nadolsky, J. Pumplin and C.-P. Yuan, “New parton distributions for collider physics,” Phys. Rev. D **82**, 074024 (2010), [arXiv:1007.2241 [hep-ph]].
  - [8] S. Chatrchyan *et al.* [CMS Collaboration], “ $J/\psi$  and  $\psi_{2S}$  production in  $pp$  collisions at  $\sqrt{s} = 7$  TeV,” JHEP **1202**, 011 (2012) [arXiv:1111.1557 [hep-ex]].
  - [9] V. Khachatryan *et al.* [CMS Collaboration], “Measurement of  $J/\psi$  and  $\psi(2S)$  Prompt Double-Differential Cross Sections in  $pp$  Collisions at  $\sqrt{s}=7$ TeV,” Phys. Rev. Lett. **114**, no. 19, 191802 (2015), [arXiv:1502.04155 [hep-ex]].
  - [10] R. Baier and R. Ruckl, “Hadronic Collisions: A Quarkonium Factory,” Z. Phys. C **19**, 251 (1983).
  - [11] B. Humpert, “Narrow Heavy Resonance Production By Gluons,” Phys. Lett. B **184**, 105 (1987).
  - [12] R. Gastmans, W. Troost and T. T. Wu, “Production of Heavy Quarkonia From Gluons,” Nucl. Phys. B **291**, 731 (1987).
  - [13] P. L. Cho and A. K. Leibovich, “Color octet quarkonia production,” Phys. Rev. D **53**, 150 (1996), [hep-ph/9505329].

- [14] P. L. Cho and A. K. Leibovich, “Color octet quarkonia production. 2.,” *Phys. Rev. D* **53**, 6203 (1996), [hep-ph/9511315].
- [15] E. Braaten, S. Fleming and A. K. Leibovich, “NRQCD analysis of bottomonium production at the Tevatron,” *Phys. Rev. D* **63**, 094006 (2001), [hep-ph/0008091].
- [16] E. J. Eichten and C. Quigg, “Mesons with beauty and charm: Spectroscopy,” *Phys. Rev. D* **49**, 5845 (1994) [hep-ph/9402210].
- [17] R. Sharma and I. Vitev, “High transverse momentum quarkonium production and dissociation in heavy ion collisions,” *Phys. Rev. C* **87**, no. 4, 044905 (2013), [arXiv:1203.0329 [hep-ph]].
- [18] D. Acosta *et al.* [CDF Collaboration], “Upsilon production and polarization in p anti-p collisions at  $\sqrt{s} = 1.8\text{-TeV}$ ,” *Phys. Rev. Lett.* **88**, 161802 (2002).
- [19] V. Khachatryan *et al.* [CMS Collaboration], “Measurement of the Inclusive Upsilon production cross section in pp collisions at  $\sqrt{s}=7\text{ TeV}$ ,” *Phys. Rev. D* **83**, 112004 (2011).
- [20] M. Butenschon and B. A. Kniehl, “Reconciling  $J/\psi$  production at HERA, RHIC, Tevatron, and LHC with NRQCD factorization at next-to-leading order,” *Phys. Rev. Lett.* **106**, 022003 (2011).
- [21] M. Butenschoen and B. A. Kniehl, “World data of J/psi production consolidate NRQCD factorization at NLO,” *Phys. Rev. D* **84**, 051501 (2011).
- [22] M. Butenschoen and B. A. Kniehl, “Probing nonrelativistic QCD factorization in polarized  $J/\psi$  photoproduction at next-to-leading order,” *Phys. Rev. Lett.* **107**, 232001 (2011).
- [23] D. Acosta *et al.* [CDF Collaboration], “Measurement of the  $J/\psi$  meson and  $b$ -hadron production cross sections in  $p\bar{p}$  collisions at  $\sqrt{s} = 1960\text{ GeV}$ ,” *Phys. Rev. D* **71**, 032001 (2005).
- [24] K. Nakamura *et al.* [Particle Data Group Collaboration], “Review of particle physics,” *J. Phys. G* **37**, 075021 (2010).